Environmental Research 303 (2026) 124791

Contents lists available at ScienceDirect

Environmental Research

journal homepage: www.elsevier.com/locate/envres

Tracking atmospheric trace elements in a historically impacted region using lichens as biomonitors: past trends and spatial contrast

Hugo Counoy [a], Zoé Matthée [a], Gustavo Ferreira Lerche [a], Laure Turcati [b], Yannick Agnan [a,*]

[a] Earth and Life Institute, Université de Louvain, Louvain-la-Neuve, 1348, Belgium
[b] Sorbonne Université, OSU Ecce Terra, 4 Place Jussieu, Paris, 75252, France

ARTICLE INFO

Keywords:
Bioaccumulation
Metals
Air pollution
Herbarium
Legacy pollutants

ABSTRACT

Atmospheric trace element contamination remains a major concern, particularly in historically industrialized regions where present-day levels reflect both ongoing emissions and legacy pollution. However, long-term trends and spatial variability are poorly constrained due to limited data and sparse monitoring networks. To address these gaps, herbarium and contemporary samples of the lichen *Xanthoria parietina* were combined to reconstruct multi-decadal trends and characterize current spatial patterns of atmospheric trace element deposition in Wallonia (southern Belgium), a region shaped by intense 19th–20th century industrialization. Comparisons between historical and contemporary samples revealed a marked but element-specific decline in enrichment. Cadmium, As, Pb, and Zn exhibited high enrichment in herbarium samples (median enrichment factor of 41–196), whereas contemporary levels were substantially lower (6–56). The largest declines (3 to 6 times lower) were observed for Pb, As, and Cd, consistent with the reduction of emissions from coal combustion and leaded gasoline. In contrast, elements such as Cu showed little temporal change, indicating the persistence of non-exhaust traffic sources. Extensive contemporary sampling revealed limited contrasts in concentrations, whereas enrichment factors showed strong anthropogenic gradients, particularly for Cd, Zn, and Pb. Positive matrix factorization further identified industrial activities, non-exhaust traffic emissions, and dust resuspension as the dominant current contributors. This dual historical–contemporary approach demonstrates the value of lichen biomonitoring for assessing atmospheric contamination in historically impacted landscapes.

1. Introduction

Air pollution remains a major environmental and public health concern worldwide, causing several million premature deaths each year, largely driven by exposure to particulate matter (PM; World Health Organization, 2021). While the adverse health effects of PM mass concentration and particle size are well established (Orellano et al., 2020; Zanobetti and Schwartz, 2009), growing evidence highlights the importance of PM chemical composition in modulating toxicity (Carvalho-Oliveira et al., 2015; Park et al., 2018). Trace elements—including metals and metalloids such as As, Cd, and Pb—embedded in airborne particles pose a major concern due to their persistence in the environment, bioaccumulative behavior, and long-term effects on ecosystems and human health (Broomandi et al., 2023; Guo et al., 2022; Jena and Singh, 2017).

These issues are especially relevant in Europe, where intense industrialization during the 19th and 20th centuries led to widespread emissions of trace elements from coal combustion, metallurgy, and heavy industry. These emissions peaked between the 1950s and the early 1980s before declining following the introduction of environmental regulations and technological improvements (Berg et al., 2008; Sen and Peucker-Ehrenbrink, 2012). Despite this decline, the legacy of historical pollution remains detectable in soils across many European regions (Binner et al., 2023; Panagos et al., 2013). However, direct information on past atmospheric trace element levels is scarce, hindering the reconstruction of long-term trends and limiting our understanding of how current exposure patterns relate to past emissions.

Beyond this historical gap, assessing atmospheric trace element contamination remains challenging. Ambient concentrations are typically low, spatially heterogeneous, and arise from complex mixtures of

This article is part of a special issue entitled: Biomonitoring environmental pollution published in Environmental Research.

* Corresponding author.
E-mail address: yannick.agnan@biogeoscience.eu (Y. Agnan).

https://doi.org/10.1016/j.envres.2026.124791
Received 28 February 2026; Received in revised form 11 May 2026; Accepted 17 May 2026
Available online 18 May 2026

diffuse and point sources, including traffic, industry, and resuspension of contaminated soils (Fakayode and Olu-Owolabi, 2003; Liu et al., 2024; Minguillón et al., 2014). Moreover, conventional instrumental monitoring relies on costly infrastructure, limiting spatial coverage, sampling density, and the number of monitored elements (Snyder et al., 2013). As a result, regulatory monitoring often provides a fragmented view of atmospheric trace element contamination, particularly outside major urban centers and industrial hotspots. This limitation is particularly critical in historically industrialized regions, where atmospheric trace element concentrations reflects the combined influence legacy soil contamination and contemporary sources, leading to pronounced spatial heterogeneity (Monaci and Baroni, 2025).

In this context, biological monitoring offers a cost-effective complement to instrumental measurements, particularly for improving spatial resolution (Schröder and Nickel, 2019; Wolterbeek, 2002). Among biomonitors, epiphytic lichens are widely used as passive samplers of atmospheric trace element deposition (Conti and Cecchetti, 2001). Their lack of roots and cuticle enables efficient accumulation of airborne elements, providing an integrated signal of atmospheric contamination over periods of months to years (Kularatne and de Freitas, 2013; Zhao et al., 2019). Owing their wide distribution across diverse environments, lichen biomonitoring supports high-density sampling and can resolve fine-scale concentration gradients, revealing localized emission sources that are not captured by sparse monitoring networks (Niepsch et al., 2024; Pollard et al., 2015; Sloof and Wolterbeek, 1991).

Beyond contemporary monitoring, historical lichen specimens preserved in herbaria offer a unique opportunity to retrospectively investigate past atmospheric contamination. Previous studies have successfully used herbarium mosses or lichens to reconstruct temporal trends in trace element deposition over several decades (Agnan et al., 2015; Minganti et al., 2014; Wu et al., 2021). However, most reconstructions have relied on specimens collected in relatively remote or environmentally protected settings (e.g. mountainous or forested areas), which primarily reflect large-scale background signals. As a result, little is known about how atmospheric trace element contamination in rural areas has evolved in the vicinity of major historical emission sources, where diffuse exposure likely persisted despite declining emissions.

In this context, the present study investigated both past and present atmospheric trace element contamination at a regional scale in Wallonia, southern Belgium, using epiphytic lichens (*Xanthoria parietina*) as biomonitors. This region constitutes a representative case study of European territories that experienced intense industrialization throughout the 19th and 20th centuries and associated high emissions of trace elements. Our objectives were twofold: (1) to reconstruct, for the first time in a historical emission hotspot, regional temporal trends of atmospheric trace element contamination in rural environments from the industrial peak (i.e., the 1950s–1980s) to the present by comparing historical herbarium specimens with contemporary samples collected at the same locations; and (2) to assess current atmospheric trace element levels and identify their dominant sources across a heterogeneous regional landscape—including urban, agricultural, and semi-natural areas—through extensive contemporary sampling. We hypothesize that, despite the overall decline in emissions, residual legacy signatures of past industrial activities may still be detectable in present-day trace element patterns, with a stronger imprint expected in urban areas.

2. Materials and methods

2.1. Study area

The study was conducted in Wallonia, southern Belgium (~16,900 km^2, ~3.7 million inhabitants), one of Europe's earliest and

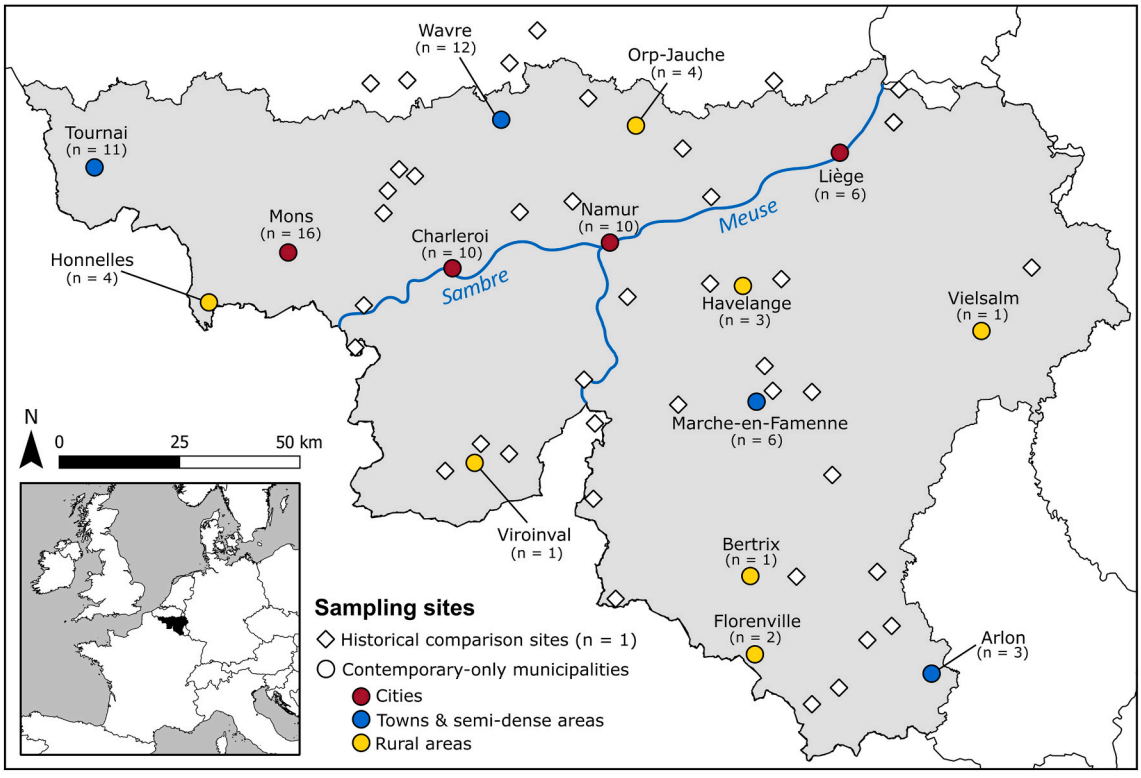

Fig. 1. Location of the 130 sampling sites of *Xanthoria parietina* in Wallonia (southern Belgium) and adjacent regions (Flanders, France, and Luxembourg), including 40 paired sites for historical comparison (i.e., historical herbarium specimens and their contemporary counterparts collected at the same locations) and 90 contemporary sampling sites grouped within 15 municipalities. "n" indicates the number of sites per municipality. Municipality categories (cities, towns and semi-dense areas, and rural areas) follow the European DEGURBA classification (European Commission, 2021).

most intensively industrialized regions (Fig. 1). From the 19th century, the region developed rapidly due to coal mining, iron and steel production, and non-ferrous metallurgy, the latter having left a marked legacy of soil contamination (Liénard and Colinet, 2016). Such activities were mainly concentrated along the Sambre–Meuse valley (i.e., a major urban–industrial corridor following the Sambre and Meuse rivers; Fig. 1), which also became the demographic and economic core of the region.

These industrial development peaked in the mid-20th century before declining with the restructuring of the metallurgical sector (Reid and Musyck, 2000). Today, the Sambre–Meuse valley still concentrates the main industrial and urban centers, notably Charleroi and Liège (Fig. 1), contrasting with the predominantly agricultural areas in the north and the sparsely populated rural and forested areas in the south.

2.2. Sampling

We used the epiphytic lichen *Xanthoria parietina* (L.) Th. Fr. as a biomonitor for this study. This choice was based on its: (1) documented tolerance to metal pollution, ensuring its survival in contaminated areas (Dzubaj et al., 2008; Pawlik-Skowrońska et al., 2002); (2) widespread occurrence across both rural and urban environments in Wallonia (Sérusiaux et al., 2004); and (3) extensive use in European biomonitoring studies, which facilitates comparative analysis (Brunialti and Frati, 2014).

To investigate both temporal trends and current regional patterns of trace element contamination, samples of this species were obtained through two complementary approaches: (1) the collection of historical herbarium specimens; and (2) a contemporary field sampling campaign.

2.2.1. Historical herbarium samples

We selected historical specimens of *Xanthoria parietina* from the herbaria of Jacques Lambinon (ULiège, Liège) and Jacques de Sloover (UCLouvain, Louvain-la-Neuve) based on sufficient biomass for chemical analysis and the availability of precise collection metadata (i.e., sampling date and location). This yielded 40 samples from rural Wallonia or its immediate vicinity (i.e., five sites in Flanders and one in northern France; Fig. 1), collected between 1959 and 1986, predominantly (70%) during 1962–1964 (detailed sample metadata in Supplementary material 1).

Throughout their conservation history, all selected specimens were stored in individual zip-lock plastic bags, ensuring homogeneous long-term storage and minimizing the risk of post-collection contamination.

2.2.2. Contemporary sampling

Contemporary sampling was conducted between 2023 and 2025, with most samples (74%) collected between May and September. At each site, three independent replicates were collected from three different trees located within a 50 m radius. For each replicate, approximately 15–20 intact *Xanthoria parietina* thalli were removed from the tree trunk at ≥1 m above ground level to minimize soil influence. Samples were collected using a ceramic knife and immediately stored in individual plastic bags to prevent metal contamination. Sites were characterized by open canopy conditions, and sampling targeted trees with a circumference >50 cm, prioritizing lime trees (*Tilia* spp.; 73%) when available, to ensure standardization and limit potential effects on bioaccumulation.

To enable temporal comparisons of trace element contamination, 40 contemporary samples were collected in 2023 at the same locations as the herbarium specimens, according to label information. To characterize present-day regional patterns of trace element contamination, the historical dataset—largely representative of rural background conditions—was complemented with an extended contemporary sampling designed to capture urban and local-scale variability across Wallonia. These sites were selected along an urbanization gradient following the DEGURBA level 1 classification (European Commission, 2021). This stratified design encompassed three distinct settlement types: (1) four major cities (Charleroi, Liège, Mons, and Namur); (2) four towns and semi-dense areas (Arlon, Marche-en-Famenne, Tournai, and Wavre); and (3) seven rural areas (Bertrix, Florenville, Havelange, Honelles, Orp-Jauche, Vielsalm, and Viroinval). The selection of those additional rural municipalities aimed to capture a representative range of the region's diverse agricultural and semi-natural areas.

Within each municipality, several sites were sampled in contrasting local environments (e.g., roadside trees, urban parks, residential neighborhoods, and industrial areas, where present) to reflect the diversity of potential emission sources. The number of sampling sites was intentionally higher in urban areas (3–10 sites) than in rural ones (1–4 sites). The exact number of sites depended on both municipality size and the local availability of suitable tree stands (i.e., groups of at least three trees hosting sufficient *Xanthoria parietina* for sampling). This resulted in a total of 90 additional contemporary sites.

2.3. Samples preparation and analytical procedure

Immediately after collection, samples were air-dried at ambient temperature (~20 °C) in a drying room for one week. Macroscopic foreign material on lichen surfaces (e.g., mosses, other lichen species, bark fragments) was removed using plastic tweezers and a ceramic knife under a stereomicroscope, without washing to preserve particulate matter trapped on the thalli (Boonpeng et al., 2021). Samples were subsequently ground to a fine powder using a ceramic mortar and pestle with liquid nitrogen.

Powdered lichen samples (typically ~100 mg; minimum 20 mg for limited herbarium specimens) were digested in Teflon vessels within an ISO 6 cleanroom (Earth and Life Institute, UCLouvain, Belgium). The digestion followed a four-step procedure adapted from Agnan et al. (2013), utilizing suprapure H_2O_2, HF, HNO_3, and HCl. Heating plate temperature was maintained at 90 °C for heating steps (at least for 48 h) and 40 °C for evaporation steps. All cleaning and analytical protocols utilized high-purity Milli-Q water (18.2 MΩ cm). Final digests were diluted 1200-fold in a 2% HNO_3 solution before analysis.

Concentrations of 15 trace elements (Al, As, Ba, Cd, Co, Cr, Cu, Fe, Mn, Ni, Pb, Sr, Ti, V, and Zn) were determined by ICP-MS (iCAP Q ICP-MS, Thermo Fisher Scientific, Waltham, MA, USA) at the Earth and Life Institute analytical platform (MOCA, UCLouvain, Belgium). Certified reference material (IAEA-336) was analyzed for quality control. The average recoveries (i.e., $C_{measured}/C_{certified} \times 100$) were within 100 ± 20% for all elements, except Ni (54%), which nonetheless showed high repeatability between analytical series. Procedural blanks (n = 2 per series) represented <1% of the mean sample concentration for all elements, except for As, Sr, and Zn (<2%). Limits of detection were <10 μg kg^{-1}, except for As, Ni, and Zn (<100 μg kg^{-1}), and Al, Fe, and Ti (<1 mg kg^{-1}). All samples showed concentrations above the analytical limits of detection for all measured elements.

2.4. Data processing and statistical analyses

For each contemporary site, mean concentrations and standard deviations were calculated from the three independent lichen subsamples and used in all subsequent analyses. Herbarium samples consisted of single composite specimens and were treated individually. Enrichment factors, multivariate analyses, and regression models were performed in R version 4.4.1 (R Core Team, 2024). Data distributions were assessed using Shapiro–Wilk tests and were non-normal; consequently, non-parametric statistical tests were applied. Differences among groups were assessed using Kruskal–Wallis tests ($\alpha = 0.05$) followed by Dunn's post hoc comparisons with Benjamini–Hochberg correction. Paired comparisons between herbarium and contemporary samples were performed using Wilcoxon signed-rank tests.

2.4.1. Enrichment factors

We calculated enrichment factors (EFs; Loska et al., 1997) to assess anthropogenic contributions. For each sample and each element X, an EF was computed using Al as a reference and normalized to the upper continental crust (UCC; Taylor and McLennan, 1985), following common practice in atmospheric deposition studies (Agnan et al., 2015; Wu et al., 2021):

$$EF_{sample}(X) = \frac{(X/Al)_{sample}}{(X/Al)_{UCC}}$$

EFs provide a standardized metric of element enrichment, allowing comparison across sites and elements while highlighting anthropogenic contributions. Values close to 1 indicate a predominantly natural origin, while values below 1 reflect depletion relative to the reference crust. Increasing EF values denote growing anthropogenic influence, with values above 10 indicating a dominant (i.e., >90%) anthropogenic contribution.

2.4.2. Source apportionment by positive matrix factorization

Source apportionment of trace element concentrations measured at the 130 contemporary sites was performed via positive matrix factorization (PMF) with the EPA PMF version 5.0 software (U.S. Environmental Protection Agency, 2014). PMF is a multivariate receptor model that decomposes the observed concentration matrix (X) into two positive matrices: factor profiles (F), representing the chemical signature of the potential emission sources, and factor contributions (G), quantifying the influence of each source at each sampling site. The PMF model can be expressed as:

$$X_{ij} = \sum_{k=1}^{p} G_{ik}F_{kj} + E_{ij}$$

where: i denotes the sampling site, j the chemical element, k the factor index, p the number of factors, and E_{ij} the residual term.

This approach enables the identification of dominant contamination sources and the assessment of their relative importance across the study area (Contardo et al., 2020; Guan et al., 2018). In PMF, the number of factors is selected by the user to balance model adequacy and interpretability while avoiding overfitting (Brown et al., 2015). A four-factor solution was selected after testing several PMF configurations, based on a multi-criteria evaluation including model goodness-of-fit (Q parameter), solution stability (bootstrap and displacement analyses), and the geochemical interpretability of the resulting factor profiles (more details in Supplementary material 2).

2.4.3. Multivariate and regression analyses

To explore relationships among elements and identify patterns in historical contamination, a principal component analysis (PCA; *FactoMineR* package) was performed on clr-transformed concentrations (*compositions* package) to account for the compositional nature of the data.

To assess the environmental consistency of the sources identified by PMF, factor contributions at each site were related to environmental variables using generalized linear mixed models (GLMMs; *lme4* package). Models were fitted with a Gamma error distribution and a log link, appropriate for positive and right-skewed factor contribution data. Candidate explanatory variables were selected to test the source-related hypotheses suggested by the PMF results. These included population density (Global Human Settlement Layer; Pesaresi et al., 2024) and land-cover proportions (i.e., artificial surfaces and croplands; CLC + Backbone; Probeck et al., 2021), calculated within a 1000 m radius circular buffer. This radius was selected as a representative compromise of the surrounding environmental context, as alternative buffer radii (500-2000 m) yielded similar results (data not shown). Additional predictors consisted of Euclidean distances (in meters) from each sampling site to major potential trace element emission sources. These included limestone quarries, industrial facilities emitting trace elements (as listed in the European Pollutant Release and Transfer Register; European Parliament, 2006), and traffic-related infrastructures (i.e., major roads and braking zones, defined as roundabouts and traffic lights) derived from OpenStreetMap. To account for dominant atmospheric transport patterns, distances were calculated both isotropically and directionally by restricting source influence to a 90° sector aligned with the prevailing south-westerly winds. All distance metrics were also log-transformed prior to modelling to account for the expected exponential decrease of concentrations with increasing distance from potential sources (Dupont et al., 2025; Wang et al., 2017).

To limit multicollinearity, Spearman's rank correlation coefficients were computed among candidate explanatory variables and between these variables and PMF factor contributions (Supplementary material 2, Fig. S1–S2), leading to the selection of five non-redundant predictors. Separate GLMMs were fitted for each PMF factor using the same set of predictors. with municipality included as a random intercept to account for the hierarchical sampling design. Residual spatial autocorrelation was assessed using Moran's I and was found to be non-significant.

3. Results and discussion

3.1. Temporal evolution of rural atmospheric trace element contamination

Results presented in this section are based on paired historical (1959–1986) and contemporary (2023) samples collected at the same locations in rural open areas.

3.1.1. Concentrations in historical comparison sites

Trace element concentrations in herbarium samples (statistical summary in Supplementary material 3) followed a decreasing order of median values: Al (5500 μg g^{-1}) > Fe > Ti > Zn > Mn > Pb > Ba > Sr > Cu > V > Cr > Ni > As > Co > Cd (1.3 μg g^{-1}). Contemporary samples exhibited lower median concentrations for all elements, with a modified ranking: Al (1900 μg g^{-1}) > Fe > Ti > Zn > Mn > Ba > Cu > Sr > Cr > Pb > V > Ni > As > Co > Cd (0.2 μg g^{-1}). Herbarium-to-contemporary ratios, calculated from paired median concentration data, were consistently >1, though their magnitudes varied among elements: ratios were low (1–3) for Al, Ba, Cr, Cu, Mn, Sr, and Ti; intermediate (3–6) for Co, Fe, Ni, V, and Zn; and reached the maximum for Cd (8.2), As (9.6), and Pb (17.0). These results indicate a strong decline in atmospheric trace element concentrations since the mid-20th century, particularly for As, Cd, and Pb, which were hallmarks of historical industrial and traffic-related emissions (Berg et al., 2008; Liang et al., 2022).

Concentrations measured in the herbarium samples exceed those reported in most previous retrospective studies conducted over comparable periods (Agnan et al., 2015; Paoli et al., 2025; Purvis et al., 2007). This difference likely reflects contrasting environmental contexts: while previous research primarily focused on lichens from remote or protected areas (e.g., forests or mountainous regions), our samples originate from rural open areas in the vicinity of a historically industrialized region.

However, these comparisons must be treated with caution. Apparent concentration shifts may partly reflect the degradation of the lichen's organic matrix over time (Agnan et al., 2014), while inter-study comparisons are further complicated by the use of different lichen species with distinct accumulation capacities (Cecconi et al., 2019; Nimis et al., 2001). Consequently, normalization and multivariate approaches are required to robustly assess temporal trends and source signatures.

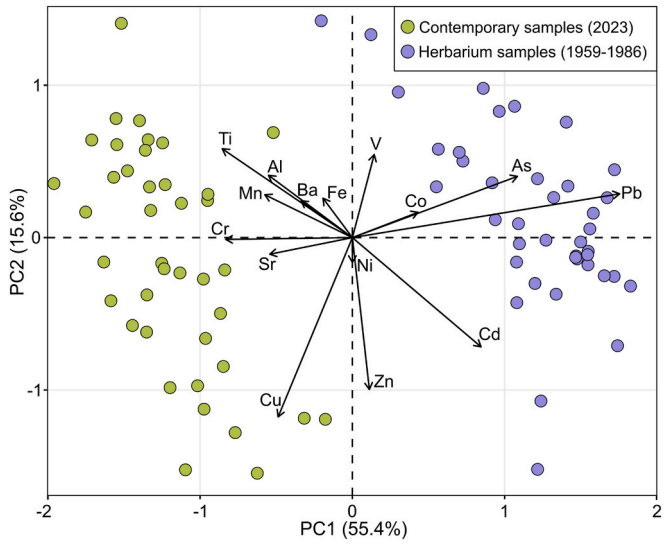

Fig. 2. Principal component analysis biplot of clr-transformed trace element concentrations in *Xanthoria parietina* from 40 historical comparison sites: herbarium (1959–1986) vs contemporary samples (2023).

3.1.2. *Elemental associations in historical comparison sites*

To explore temporal patterns in relative trace element composition, we performed a PCA on paired herbarium and contemporary samples (Fig. 2). The first two axes explained 71.0% of the total variance. The first axis (PC1, 55.4%) clearly separated herbarium samples (positive scores) from contemporary samples (negative scores). Elements with high positive loadings on PC1 (i.e., As, Cd, and Pb) are characteristic of historical industrial emissions from coal combustion and non-ferrous metallurgy (Sen and Peucker-Ehrenbrink, 2012), with Pb further reflecting the legacy of leaded gasoline (von Storch et al., 2003). Conversely, elements with negative loadings (i.e., Ti, Cr, Al, Cu, Sr, and Mn) are typically linked to lithogenic or mixed-origin inputs (Rauch and Pacyna, 2009; Sen and Peucker-Ehrenbrink, 2012). PC1 thus captures a temporal shift, with herbarium samples showing strong anthropogenic enrichment, whereas contemporary samples reflect a greater relative contribution of lithogenic elements as industrial signatures decline.

The second axis (PC2; 15.6%) reflected spatial variability rather than temporal differences. It opposed lithogenic tracers (i.e., Ti and V; Nriagu, 1989; Sen and Peucker-Ehrenbrink, 2012) to elements associated with industrial and traffic-related sources (i.e., Zn, Cu, and Cd; Councell et al., 2004; Denier van der Gon et al., 2007). Interestingly, paired samples from the same location generally occupied similar positions along PC2 (labels not shown for clarity). Although a small but significant mean shift was detected (i.e., with contemporary samples scoring 0.27 ± 0.76 units lower; paired *t*-test, $p < 0.05$), this was negligible compared to the overall axis dispersion. This suggests that spatial contrasts among sites have remained largely consistent over the decades.

Overall, the PCA results distinguished between legacy-dominated elements (As, Pb), whose influence has collapsed over time, and persistent elements (Cu, Zn), whose spatial patterns endure. However, some elements such as Cd exhibited intermediate behavior, contributing to both the dominant temporal contrast and the persistent spatial gradient.

3.1.3. *Enrichment factors in historical comparison sites*

To quantify changes in the magnitude of anthropogenic enrichment over time, enrichment factors (EFs) were calculated for both historical

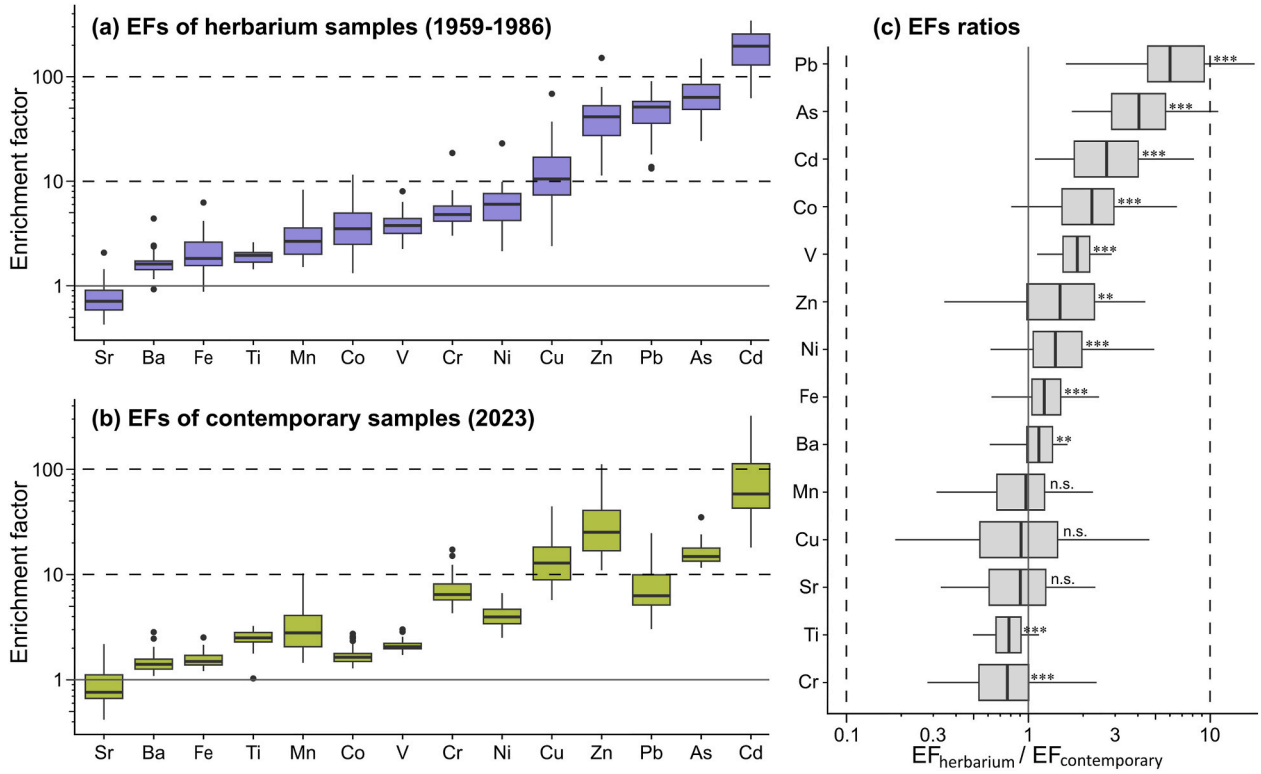

Fig. 3. Enrichment factors (EFs) of trace elements in *Xanthoria parietina* from the 40 paired historical comparison sites. Panels (a) and (b) show the distribution of EFs for herbarium (1959–1986) and contemporary (2023) samples, respectively. Panel (c) shows the distribution of the paired ratios ($EF_{herbarium}/EF_{contemporary}$) calculated for each of the 40 historical comparison sites. EF ratios >1 indicate higher anthropogenic enrichment in the past, while ratios <1 indicate higher enrichment at present. Stars indicate statistically significant differences between herbarium and contemporary EFs based on Wilcoxon signed-rank tests (*$p < 0.05$, **$p < 0.01$, ***$p < 0.001$).

and contemporary samples (Fig. 3; statistical summary in Supplementary material 3). In herbarium specimens, Cd (median EF = 196), As (64), Pb (51), and Zn (41) exhibited consistently high enrichment factors (EF > 10 at all sites), reflecting the intense anthropogenic pressure during the mid-20th century (Fig. 3a). Moderate enrichment (median EF = 5–10) was observed for Cu, Cr, and Ni, while Sr was the only element with a median EF slightly below 1, confirming its predominantly lithogenic origin.

In contemporary samples, EFs were generally lower and displayed a reconfigured relative ranking (Fig. 3b). Cadmium remained the most enriched element (median EF = 56), followed by Zn, As, Cu, Cr, and Pb (median EF = 6–24). Paired comparisons revealed significantly higher enrichment in herbarium samples for most elements ($p < 0.05$). Conversely, no significant temporal change was observed for Cu, Mn, and Sr, while Ti and Cr exhibited slightly higher median EFs in the contemporary samples ($p < 0.05$), although Ti remained near baseline levels (EF close to 2) and Cr only occasionally approached EF of 10.

The magnitude of these shifts, summarized by herbarium-to-contemporary EF ratios (Fig. 3c), showed the most pronounced declines for Pb (median ratio of 6.1), As (4.0), Cd (2.6), and Co (2.2). These trends align with the broad European emission reductions (Purvis et al., 2007; Wu et al., 2021). However, our results highlighted regional specificities: unlike previous studies in rural western France that found stable Cd and Zn levels (Agnan et al., 2015), our data showed significant declines for both. This suggests the concomitant influence of: (1) a widespread background atmospheric signal linked to historical coal combustion and leaded gasoline (Petit et al., 2015); and (2) a distinct regional signature associated with intense industrial legacy.

Despite this general decline, the persistent enrichment of several elements raises a critical question of whether present-day atmospheric inputs are driven by ongoing emissions or by the secondary remobilization of historically contaminated soils. Resolving this requires extending the spatial scope to urban and industrial hotspots, where contemporary sources can be more precisely constrained.

3.2. Contemporary spatial patterns and source apportionment of atmospheric trace elements

Results presented in this section are based on the complete present-day dataset (2023–2025), including the 40 contemporary samples from the historical comparison sites complemented by 90 additional urban and rural sites distributed across Wallonia (Fig. 1).

3.2.1. Concentrations in contemporary sites

Contemporary lichen samples showed substantial variability in trace element concentrations across sampling sites (statistical summary in Supplementary material 3). Median concentrations followed a similar order to that observed in the contemporary rural samples used for historical comparison, but were lower for all elements, ranging from 1100 $\mu g\, g^{-1}$ (Al) to 0.1 $\mu g\, g^{-1}$ (Cd). More specifically, lithogenic elements (e.g., Al, Ba, Ti, and V) were 1.5- to 2-fold higher in rural sites, whereas anthropogenic elements (e.g., Cd, Cu, Pb, and Zn) showed similar median concentrations across urban and rural areas. More pronounced contrasts emerged at the municipal scale: Liège and Charleroi, the two most densely populated and industrialized cities, showed elevated Cd, Pb, and Zn levels, with median values 1.3- to 2.8-fold higher than rural sites.

To further interpret these concentrations, we used the naturality/alteration scale proposed by Bargagli and Nimis (2002), which classifies sites based on their deviation from natural background concentrations. More than half of the contemporary samples fell within the "high" or "very high naturality" classes for anthropogenic elements (i.e., Cd, Cu, Ni, Pb, and Zn). In contrast, lithogenic or mixed-origin elements (i.e., Al, Ba, Cr, and Fe) showed higher proportion of sites (>25%) classified as "high" to "very high alteration". This apparent discrepancy highlights the limitations of using absolute concentration thresholds to detect anthropogenic influence and motivates the use of enrichment factors (Cecconi et al., 2019; Garty and Garty-Spitz, 2015).

3.2.2. Enrichment factors in contemporary sites

At the municipal scale, EFs (statistical summary in Supplementary material 3) revealed a clear anthropogenic gradient from industrial cities (i.e., Liège and Charleroi) to other urban areas and to rural sites (Fig. 4). This gradient affected not only typical anthropogenic elements (e.g., Cd, Zn, and Pb) but also several elements of mixed origin (e.g., Fe, Co, and V). Although these differences were not always statistically significant, this pattern suggests that major industrial activities, rather than urbanization alone, remain the primary driver of present-day atmospheric enrichment.

Notably, for Cd, Zn, and Pb, current EFs in Liège and Charleroi were of the same order of magnitude as those observed in rural herbarium samples from the 1950s–1980s. This indicates that current anthropogenic contributions in industrial areas remain comparable to historical levels previously observed in rural environments during the industrial peak. In contrast, As did not follow this industrial gradient. EFs remained consistently high across all contemporary sites (EF > 10; Fig. 4), but median values were approximately twofold lower than in historical rural samples (Fig. 3a). This pattern suggests a decline in primary As emissions (Zevenhoven et al., 2007), while indicating that present-day As is likely dominated by spatially diffuse sources. This may include the resuspension of legacy-contaminated soils (Monaci and Baroni, 2025; Vandeuren et al., 2023).

EFs also revealed site-specific metallurgical fingerprints. Charleroi showed higher median Ni and Cr enrichment than Liège (Fig. 4), likely reflecting its specialization in stainless steel production and scrap recycling, processes known to release these elements during alloy formulation and handling (Liu et al., 2024; Pokorná et al., 2016). Consistently, such metallurgical activities have largely ceased in Liège since the early 2010s, a trend corroborated by recent air quality monitoring (ISSeP, 2024). These findings illustrate that industrial cities are not a homogeneous category.

Similarly, rural sites displayed substantial spatial variability, with some exhibiting Cd and Zn enrichments comparable to industrial cities (Fig. 4). Among the highest values, some sites (e.g., Feluy, Mariembourg, and Saint-Remy) showed EFs ranging from 182 to 325 for Cd and from 63 to 105 for Zn. The first two sites are located a few hundred meters downwind of industrial areas, while the latter is situated in close proximity to a slag heap, suggesting the influence of localized current or legacy sources. Overall, these results show that present-day atmospheric trace element enrichment is shaped not only by the presence of major industrial centers but also by element-specific behaviors and local source configurations (Monaci and Baroni, 2025). This heterogeneity highlights the need of source apportionment approaches to disentangle industrial, urban, and lithogenic contributions.

3.2.3. Source apportionment in contemporary sites

The PMF resulted in a four-factor solution representing the main sources of present-day atmospheric trace elements at the regional scale. The chemical profiles of these factors (Fig. 5a) form the basis for source attribution, while their contributions quantify the relative importance of each source across sampling sites. When averaged by municipality (Fig. 5b), these contributions revealed spatial patterns that align with source profiles, providing a coherent assessment of both source identity and spatial influence.

To validate the environmental plausibility of these sources, factor contributions were related to environmental variables using GLMMs. Following the preliminary screening (Supplementary material SM2, Fig. S2–S3), five environmental predictors were retained: proportion of

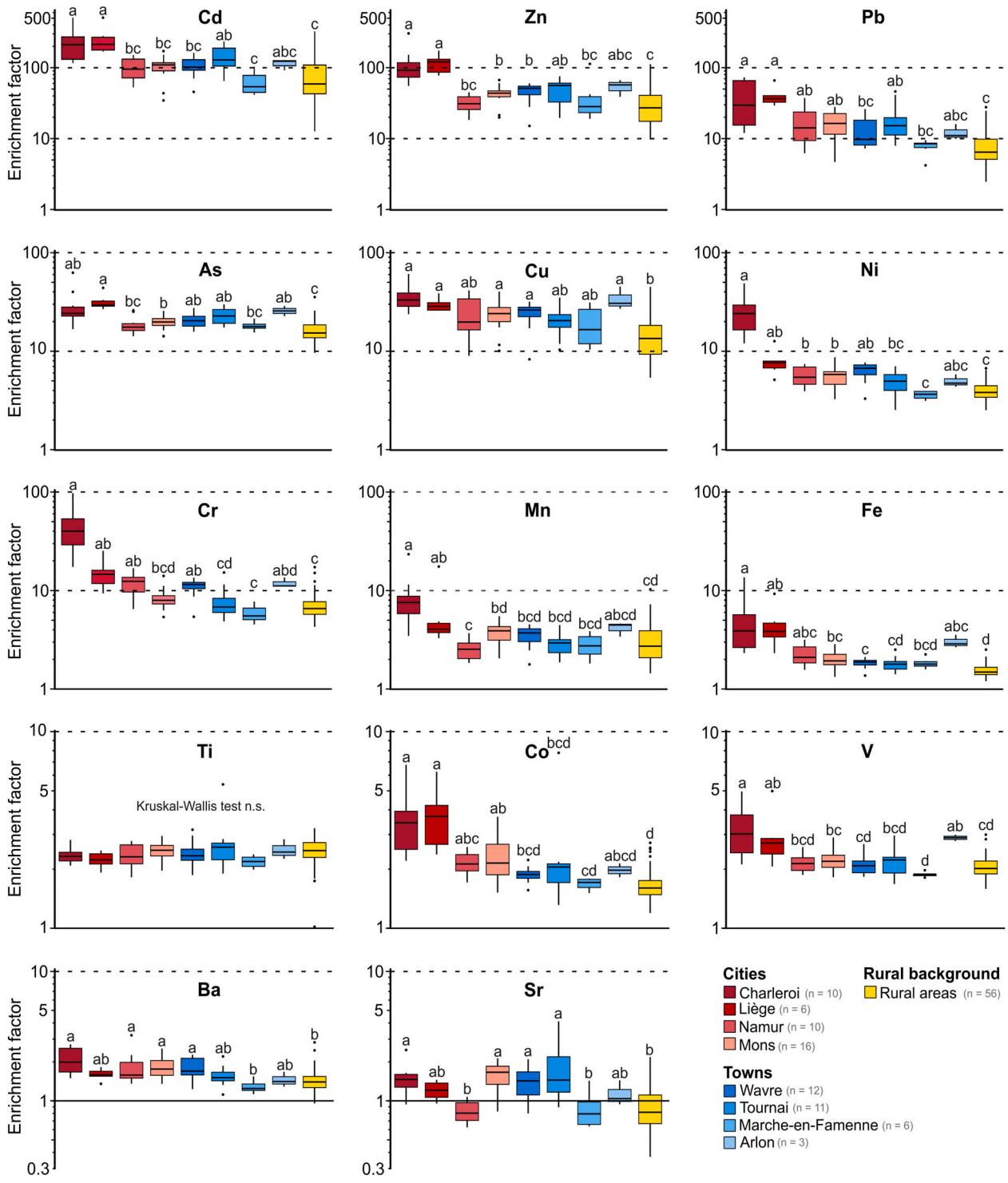

Fig. 4. Enrichment factor (EFs) of trace elements in *Xanthoria parietina* from 130 contemporary sites distributed across eight municipalities and rural areas. Groups labelled by a different letter are significantly different (Dunn's post hoc test following Kruskal–Wallis, $p < 0.05$). For Ti, no significant differences among municipalities were detected (Kruskal–Wallis test, n.s.), and no post hoc comparisons are shown. The y-axis is displayed on a logarithmic scale for all elements; y-axis ranges are shared within rows but differ within columns to reflect element-specific EF distributions.

cropland (1 km radius), distance to the nearest limestone quarry, distance to the nearest industrial facility emitting trace elements, distance to the nearest major road, and distance to the nearest braking area (i.e., roundabouts or traffic lights). Standardized regression coefficients (Table 1) were used to assess the direction and relative strength of these effects.

Factor 1 accounted for a dominant share of Pb (73%) and substantial contribution to Cd, Fe, Cr, Ni, and Zn (>35%; Fig. 5a). This composition is consistent with metallurgical and urban-industrial sources (Pacyna and Pacyna, 2001). This factor represented the highest relative contribution in Charleroi and Liège (~58%; Fig. 5b). GLMM results supported this interpretation, with a significant negative relationship with distance

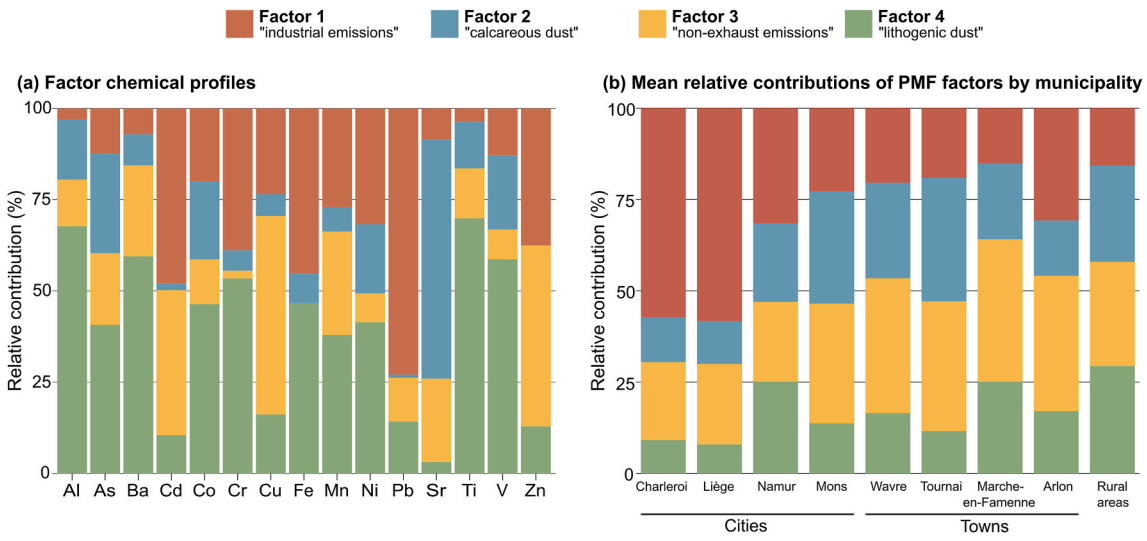

Fig. 5. Results of the positive matrix factorization (PMF) analysis: (a) chemical profiles of the four PMF factors, expressed as their relative contributions to the reconstructed concentrations of each element, and (b) mean relative contributions of the four factors to the total reconstructed trace element concentrations across municipalities.

Table 1
Standardized fixed-effect coefficients from the generalized linear mixed models relating PMF factor contributions to five environmental predictors: proportion of agricultural land within a 1 km radius, downwind distance to the nearest limestone quarry, downwind distance to the nearest industrial facility emitting trace elements, distances to the nearest major road, and distance to the nearest braking area (i.e., roundabouts or traffic lights). All predictors were centered and scaled prior to analysis to allow for a direct comparison of their relative effects within each model. Stars indicate the significance level of each coefficient (*p < 0.05, **p < 0.01, ***p < 0.001).

Model	Proportion of cropland	Downwind distance to limestone quarry	Downwind distance to industrial facility	Distance to major road	Distance to braking zone
Factor 1 *industrial emissions*	0.11	0.04	−0.31***	−0.12	−0.17*
Factor 2 *calcareous dust*	0.10	−0.01	−0.08	−0.17**	0.08
Factor 3 *non-exhaust emissions*	−0.02	0.00	0.05	−0.06	−0.16**
Factor 4 *lithogenic dust*	0.17*	0.12	0.04	−0.30***	−0.07

to industrial facilities (Table 1). A weaker but significant negative association with braking areas (Table 1) likely reflects the spatial overlap of industry and dense urban infrastructure in Charleroi and Liège—where braking zones, roads, and industrial sites are closely interwoven—rather than traffic-related source. Interestingly, while EFs captured the distinct industrial fingerprints between Liège and Charleroi based on their metallurgical history, the PMF industrial factor merged them into a singular source profile. This contrast underscores the complementarity of the two methods: EFs provide high resolution for specific tracers, whereas PMF identifies broader, multi-elemental source contributions (Dörter et al., 2020; Guan et al., 2018; Wu et al., 2021).

Factor 2 was the primary contributor to reconstructed Sr concentrations (66%; Fig. 5a), with secondary contributions to As, Co, and V. Given the predominantly lithogenic nature of Sr (i.e., low EFs; Fig. 4) and its strong association with carbonate minerals (Pathak et al., 2020), Factor 2 likely reflects a calcareous dust signal (Purvis et al., 2005). Spatially, its relative contributions peaked in Tournai (34%; Fig. 5b), a municipality hosting several large limestone quarries with a combined annual production exceeding 20 million tons (Tshibangu et al., 2004). Notably, one site located less than 1 km downwind of a major quarry showed a particularly high contribution of this factor (73%), supporting a local carbonate dust influence. However, GLMM results showed no significant relationship with quarry proximity despite weak effects in the expected directions (Table 1). This lack of statistical significance likely reflects the diffuse and highly variable nature of carbonate dust emissions, which depends more on site-specific operational conditions and dust mitigation practices than on simple distance- or land-cover-based predictors.

Factor 3 was characterized by strong contributions to Cu (54%), Zn (50%), and Cd (39%), a profile typical of non-exhaust traffic emissions (Fig. 5a; Duong and Lee, 2011; Mastin et al., 2023; Wang et al., 2017). Copper is primarily associated with brake wear (i.e., >50% of atmospheric Cu emissions in Western Europe; Denier van der Gon et al., 2007), while Zn is released through tire wear and road surface abrasion (Councell et al., 2004; Gustafsson et al., 2008). Although distinct, these two processes occur simultaneously during braking, leading PMF to group them into a single factor. GLMMs further supported this source attribution, with Factor 3 showing a significant negative relationship with distance to braking areas (Table 1). These findings align with the historical patterns captured by PC2 (Fig. 2), indicating a stable, long-term spatial imprint of non-exhaust emissions.

Factor 4 contributed mainly to Al and Ti (~70%), and to a lesser extent to As, Ba, Co, Cr, Fe, Ni, Mn, and V (35-60%), clearly identifying a lithogenic source dominated by soil-derived particles (Fig. 5a). GLMM results further support this interpretation, showing a significant positive association with cropland proportion, consistent with enhanced dust resuspension from farming activities (Chen et al., 2023; Zhang et al., 2025). The substantial contribution of this factor to As (Fig. 5a) suggests that present-day atmospheric As is largely associated with soil-derived material, potentially reflecting a combination of natural background and the remobilization of legacy contamination, a hypothesis supported by the persistently high EFs (>10) across all sites (Fig. 4) and the past

rural contamination of this element (Fig. 3). However, disentangling current emissions from legacy contamination remains challenging and would require complementary approaches such as isotopic ratios or specific geochemical tracers (Agnan et al., 2014; Graney et al., 2017; Véron et al., 1999).

Interestingly, both dust-related factors (Factors 2 and 4) showed significant negative associations with distance to major roads (Table 1). This suggests that roads act not as primary sources, but as drivers of particle resuspension via vehicle-induced turbulence (Rienda and Alves, 2021; Vern, 2022). These results highlight a shift in traffic-related impacts, from historically dominant exhaust emissions (e.g., Pb), to non-exhaust processes (i.e., brake and tire wear; Factor 3) and soil dust resuspension (Factors 2 and 4).

In conclusion, the combined PMF-GLMMs approach demonstrates that present-day atmospheric trace element patterns across Wallonia result from a complex interplay of persistent industrial emissions, widespread traffic sources, and heterogeneous dust inputs. While GLMMs effectively corroborate industrial and traffic attributions, dust-dominated factors remain less constrained due to their diffuse nature and dependence on local soil-use dynamics.

4. Conclusions

By combining herbarium lichen specimens with an extensive contemporary sampling, this study substantially improved the temporal depth and spatial resolution of atmospheric trace element assessment in a historically industrialized region.

Historical comparison documented a substantial, yet element-specific, decline in regional rural atmospheric contamination since the mid-20th century. Pronounced decreases were observed for elements linked to legacy diffuse sources (i.e., coal combustion and leaded gasoline), whereas industrial and non-exhaust traffic emissions showed little to no decline, indicating the persistence of these sources despite broader pollution reduction efforts.

Analysis of contemporary samples across urban and rural environments further revealed pronounced spatial heterogeneity in present-day trace element patterns. EFs, PMF, and GLMMs consistently identified industrial activities, non-exhaust traffic emissions, and both carbonate-rich and lithogenic dust as the dominant contributors, with their relative importance varying significantly between municipalities. A key finding is that modern traffic-related impacts are primarily driven by non-exhaust processes and the resuspension of soil-derived particles rather than fuel combustion.

Overall, these findings demonstrate that lichen biomonitoring is a robust approach for assessing atmospheric trace element contamination across heterogeneous and historically contaminated landscapes, provided that concentration data are interpreted beyond absolute values. The combined use of EFs and multivariate source apportionment proved essential for disentangling present-day sources and their spatial footprints. However, distinguishing ongoing emissions from the remobilization of legacy contamination remains challenging. Future studies could address this by combining lichen biomonitoring with complementary approaches, such as isotopic signatures or rare earth elements applied at selected sites.

Funding

This work was supported by Fonds pour la Formation à la Recherche dans l'Industrie et dans l'Agriculture (FRIA) from the Fonds de la Recherche Scientifique (F.R.S.-FNRS).

CRediT authorship contribution statement

Hugo Counoy: Conceptualization, Formal analysis, Funding acquisition, Investigation, Methodology, Validation, Visualization, Writing – original draft. **Zoé Matthée:** Conceptualization, Formal analysis, Investigation, Methodology, Writing – review & editing. **Gustavo Ferreira Lerche:** Formal analysis, Investigation, Methodology, Writing – review & editing. **Laure Turcati:** Supervision, Writing – review & editing. **Yannick Agnan:** Conceptualization, Funding acquisition, Methodology, Supervision, Visualization, Writing – review & editing.

Declaration of competing interest

The authors declare that they have no known competing financial interests or personal relationships that could have appeared to influence the work reported in this paper.

Acknowledgements

We thank the collectors of the herbarium specimens—C. Adams, J. Margot, M. Lambert, R. Schumacker, E. Sérusiaux, and especially J. Lambinon and J. de Sloover—for building the collections without which this study would not have been possible. We are also grateful to Nicolas Magain (ULiège), Laurent Gohy (ULiège), and Anne-Laure Jacquemart (UCLouvain) for granting access to herbarium material, Louis le Hardÿ de Beaulieu for permission to conduct lichen sampling on his property, and Laurence Monin (MOCA, UCLouvain) for ICP-MS analyses. We sincerely thank the two anonymous reviewers for their insightful comments, which improved this manuscript.

Appendix A. Supplementary data

Supplementary data to this article can be found online at https://doi.org/10.1016/j.envres.2026.124791.

References

Agnan, Y., Séjalon-Delmas, N., Claustres, A., Probst, A., 2015. Investigation of spatial and temporal metal atmospheric deposition in France through lichen and moss bioaccumulation over one century. Sci. Total Environ. 529, 285–296. https://doi.org/10.1016/j.scitotenv.2015.05.083.

Agnan, Y., Séjalon-Delmas, N., Probst, A., 2013. Comparing early twentieth century and present-day atmospheric pollution in SW France: a story of lichens. Environ. Pollut. 172, 139–148. https://doi.org/10.1016/j.envpol.2012.09.008.

Agnan, Y., Séjalon-Delmas, N., Probst, A., 2014. Origin and distribution of rare earth elements in various lichen and moss species over the last century in France. Sci. Total Environ. 487, 1–12. https://doi.org/10.1016/j.scitotenv.2014.03.132.

Guidelines for the use of epiphytic lichens as biomonitors of atmospheric deposition of trace elements. In: Bargagli, R., Nimis, P.L. (Eds.), 2002. Monitoring with Lichens — Monitoring Lichens. Kluwer/NATO Science Series. Springer, Netherlands, Dordrecht, pp. 295–299. https://doi.org/10.1007/978-94-010-0423-7.

Berg, T., Aas, W., Pacyna, J., Uggerud, H.T., Vadset, M., 2008. Atmospheric trace metal concentrations at Norwegian background sites during 25 years and its relation to European emissions. Atmos. Environ. 42, 7494–7501. https://doi.org/10.1016/j.atmosenv.2008.05.020.

Binner, H., Sullivan, T., Jansen, M.A.K., Mc Namara, M.E., 2023. Metals in urban soils of Europe: a systematic review. Sci. Total Environ. 854, 158734. https://doi.org/10.1016/j.scitotenv.2022.158734.

Boonpeng, C., Sangiamdee, D., Noikrad, S., Boonpragob, K., 2021. Influence of washing thalli on element concentrations of the epiphytic and epilithic lichen Parmotrema tinctorum in the tropic. Environ. Sci. Pollut. Res. 28, 9723–9730. https://doi.org/10.1007/s11356-020-11459-8.

Broomandi, P., Rodríguez-Seijo, A., Janatian, N., Fathian, A., Tleuken, A., Mohammadpour, K., Galán-Madruga, D., Jahanbakhshi, A., Kim, J.R., Satyanaga, A., Bagheri, M., Morawska, L., 2023. Health risk assessment of the European inhabitants exposed to contaminated ambient particulate matter by potentially toxic elements. Environ. Pollut. 323, 121232. https://doi.org/10.1016/j.envpol.2023.121232.

Brown, S.G., Eberly, S., Paatero, P., Norris, G.A., 2015. Methods for estimating uncertainty in PMF solutions: examples with ambient air and water quality data and guidance on reporting PMF results. Sci. Total Environ. 518–519, 626–635. https://doi.org/10.1016/j.scitotenv.2015.01.022.

Brunialti, G., Frati, L., 2014. Bioaccumulation with lichens: the Italian experience. Int. J. Environ. Stud. 71, 15–26. https://doi.org/10.1080/00207233.2014.880996.

Carvalho-Oliveira, R., Pires-Neto, R.C., Bustillos, J.O.V., Macchione, M., Dolhnikoff, M., Saldiva, P.H.N., Garcia, M.L.B., 2015. Chemical composition modulates the adverse effects of particles on the mucociliary epithelium. Clinics 70, 706–713. https://doi.org/10.6061/clinics/2015(10)09.

Cecconi, E., Fortuna, L., Benesperi, R., Bianchi, E., Brunialti, G., Contardo, T., Di Nuzzo, L., Frati, L., Monaci, F., Munzi, S., Nascimbene, J., Paoli, L., Ravera, S., Vannini, A., Giordani, P., Loppi, S., Tretiach, M., 2019. New interpretative scales for

lichen bioaccumulation data: the italian proposal. Atmosphere 10, 136. https://doi.org/10.3390/atmos10030136.
Chen, S., Chen, J., Zhang, Y., Lin, J., Bi, H., Song, H., Chen, Y., Lian, L., Liu, C., Zhang, R., 2023. Anthropogenic dust: sources, characteristics and emissions. Environ. Res. Lett. 18, 103002. https://doi.org/10.1088/1748-9326/acf479.
Contardo, T., Vannini, A., Sharma, K., Giordani, P., Loppi, S., 2020. Disentangling sources of trace element air pollution in complex urban areas by lichen biomonitoring. A case study in Milan (Italy). Chemosphere 256, 127155. https://doi.org/10.1016/j.chemosphere.2020.127155.
Conti, M.E., Cecchetti, G., 2001. Biological monitoring: lichens as bioindicators of air pollution assessment - a review. Environ. Pollut. 471–492. https://doi.org/10.1016/S0269-7491(00)00224-4.
Councell, T.B., Duckenfield, K.U., Landa, E.R., Callender, E., 2004. Tire-wear particles as a source of zinc to the environment. Environ. Sci. Technol. 38, 4206–4214. https://doi.org/10.1021/es034631f.
Denier van der Gon, H.A.C., Hulskotte, J.H.J., Visschedijk, A.J.H., Schaap, M., 2007. A revised estimate of copper emissions from road transport in UNECE-Europe and its impact on predicted copper concentrations. Atmos. Environ. 41, 8697–8710. https://doi.org/10.1016/j.atmosenv.2007.07.033.
Dörter, M., Karadeniza, H., Saklangıç, U., Yenisoy-Karakaş, S., 2020. The use of passive lichen biomonitoring in combination with positive matrix factor analysis and stable isotopic ratios to assess the metal pollution sources in throughfall deposition of Bolu plain, Turkey. Ecol. Indic. 113, 106212. https://doi.org/10.1016/j.ecolind.2020.106212.
Duong, T.T.T., Lee, B.-K., 2011. Determining contamination level of heavy metals in road dust from busy traffic areas with different characteristics. J. Environ. Manag. 92, 554–562. https://doi.org/10.1016/j.jenvman.2010.09.010.
Dupont, J., Ponton, D.E., Marois, A., Fenton, N.J., Amyot, M., Rosabal, M., 2025. Elemental atmospheric deposition around North America's largest metal processor of electronic waste (Horne Smelter, Canada). Front. Environ. Chem. 6, 1505053. https://doi.org/10.3389/fenvc.2025.1505053.
Dzubaj, A., Bačkor, M., Tomko, J., Peli, E., Tuba, Z., 2008. Tolerance of the lichen Xanthoria parietina (L.) Th. Fr. to metal stress. Ecotoxicol. Environ. Saf. 70, 319–326. https://doi.org/10.1016/j.ecoenv.2007.04.002.
European Commission, 2021. Applying the Degree of Urbanisation: a Methodological Manual to Define Cities, Towns and Rural Areas for International Comparisons - 2021 Edition. Publications Office of the European Union, Luxembourg.
European Parliament, 2006. Regulation (EC) No 166/2006 of the European Parliament and of the Council of 18 January 2006 Concerning the Establishment of a European Pollutant Release and Transfer Register and Amending Council Directives 91/689/EEC and 96/61/EC. Official Journal of the European Union.
Fakayode, S.O., Olu-Owolabi, B.I., 2003. Heavy metal contamination of roadside topsoil in Osogbo, Nigeria: its relationship to traffic density and proximity to highways. Environ. Geol. 44, 150–157. https://doi.org/10.1007/s00254-002-0739-0.
Garty, J., Garty-Spitz, R.L., 2015. Lichens and particulate matter: inter-relations and biomonitoring with lichens. In: Upreti, D.K., Divakar, P.K., Shukla, V., Bajpai, R. (Eds.), Recent Advances in Lichenology. Springer, India, New Delhi, pp. 47–85. https://doi.org/10.1007/978-81-322-2181-4_3.
Graney, J.R., Landis, M.S., Puckett, K.J., Studabaker, W.B., Edgerton, E.S., Legge, A.H., Percy, K.E., 2017. Differential accumulation of PAHs, elements, and Pb isotopes by five lichen species from the Athabasca oil sands region in Alberta, Canada. Chemosphere 184, 700–710. https://doi.org/10.1016/j.chemosphere.2017.06.036.
Guan, Q., Wang, F., Xu, C., Pan, N., Lin, J., Zhao, R., Yang, Y., Luo, H., 2018. Source apportionment of heavy metals in agricultural soil based on PMF: a case study in Hexi Corridor, northwest China. Chemosphere 193, 189–197. https://doi.org/10.1016/j.chemosphere.2017.10.151.
Guo, F., Tang, M., Wang, X., Yu, Z., Wei, F., Zhang, X., Jin, M., Wang, J., Xu, D., Chen, Z., Chen, K., 2022. Characteristics, sources, and health risks of trace metals in PM2.5. Atmos. Environ. 289, 119314. https://doi.org/10.1016/j.atmosenv.2022.119314.
Gustafsson, M., Blomqvist, G., Gudmundsson, A., Dahl, A., Swietlicki, E., Bohgard, M., Lindbom, J., Ljungman, A., 2008. Properties and toxicological effects of particles from the interaction between tyres, road pavement and winter traction material. Sci. Total Environ. 393, 226–240. https://doi.org/10.1016/j.scitotenv.2007.12.030.
ISSeP, 2024. Réseaux De Surveillance De La Qualité De L'Air - Rapport 2024. Institut Scientifique de Service Public (ISSeP), Liège.
Jena, S., Singh, G., 2017. Human health risk assessment of airborne trace elements in Dhanbad, India. Atmos. Pollut. Res. 8, 490–502. https://doi.org/10.1016/j.apr.2016.12.003.
Kularatne, K.I.A., de Freitas, C.R., 2013. Epiphytic lichens as biomonitors of airborne heavy metal pollution. Environ. Exp. Bot. 88, 24–32. https://doi.org/10.1016/j.envexpbot.2012.02.010.
Liang, M., Liu, E., Wang, X., Zhang, Q., Xu, J., Ji, M., Zhang, E., 2022. Historical trends in atmospheric metal(loid) contamination in North China over the past half-millennium reconstructed from subalpine lake sediment. Environ. Pollut. 304, 119195. https://doi.org/10.1016/j.envpol.2022.119195.
Liénard, A., Colinet, G., 2016. Assessment of vertical contamination of Cd, Pb and Zn in soils around a former ore smelter in Wallonia, Belgium. Environ. Earth Sci. 75, 1322. https://doi.org/10.1007/s12665-016-6137-9.
Liu, X., Zhang, X., Wang, T., Jin, B., Wu, L., Lara, R., Monge, M., Reche, C., Jaffrezo, J.-L., Uzu, G., Dominutti, P., Darfeuil, S., Favez, O., Conil, S., Marchand, N., Castillo, S., de la Rosa, J.D., Stuart, G., Eleftheriadis, K., Diapouli, E., Gini, M.I., Nava, S., Alves, C., Wang, X., Xu, Y., Green, D.C., Beddows, D.C.S., Harrison, R.M., Alastuey, A., Querol, X., 2024. PM10-bound trace elements in pan-European urban atmosphere. Environ. Res. 260, 119630. https://doi.org/10.1016/j.envres.2024.119630.
Loska, K., Cebula, J., Pelczar, J., Wiechuła, D., Kwapuliński, J., 1997. Use of enrichment, and contamination factors together with geoaccumulation indexes to evaluate the content of Cd, Cu, and Ni in the Rybnik water reservoir in Poland. Water. Air. Soil Pollut. 93, 347–365. https://doi.org/10.1007/BF02404766.
Mastin, J., Saini, A., Schuster, J.K., Harner, T., Dabek-Zlotorzynska, E., Celo, V., Gaga, E. O., 2023. Trace metals in global air: first results from the GAPS and GAPS megacities networks. Environ. Sci. Technol. 57, 14661–14673. https://doi.org/10.1021/acs.est.3c05733.
Minganti, V., Drava, G., De Pellegrini, R., Modenesi, P., Malaspina, P., Giordani, P., 2014. Temporal trends (1981–2007) of trace and rare earth elements in the lichen Cetraria islandica (L.) Ach. from Italian herbaria. Chemosphere 99, 180–185. https://doi.org/10.1016/j.chemosphere.2013.10.067.
Minguillón, M.C., Cirach, M., Hoek, G., Brunekreef, B., Tsai, M., de Hoogh, K., Jedynska, A., Kooter, I.M., Nieuwenhuijsen, M., Querol, X., 2014. Spatial variability of trace elements and sources for improved exposure assessment in Barcelona. Atmos. Environ. 89, 268–281. https://doi.org/10.1016/j.atmosenv.2014.02.047.
Monaci, F., Baroni, D., 2025. Atmospheric deposition of potentially toxic elements in a peri-urban industrial landscape: evaluating legacy vs. current pollution. Urban Clim. 64, 102685. https://doi.org/10.1016/j.uclim.2025.102685.
Niepsch, D., Clarke, L.J., Jones, R.G., Tzoulas, K., Cavan, G., 2024. Lichen biomonitoring to assess spatial variability, potential sources and human health risks of polycyclic aromatic hydrocarbons (PAHs) and airborne metal concentrations in Manchester (UK). Environ. Monit. Assess. 196, 379. https://doi.org/10.1007/s10661-024-12522-4.
Nimis, P.L., Andreussi, S., Pittao, E., 2001. The performance of two lichen species as bioaccumulators of trace metals. Sci. Total Environ. 275, 43–51. https://doi.org/10.1016/S0048-9697(00)00852-4.
Nriagu, J.O., 1989. A global assessment of natural sources of atmospheric trace metals. Nature 338, 47–49. https://doi.org/10.1038/338047a0.
Orellano, P., Reynoso, J., Quaranta, N., Bardach, A., Ciapponi, A., 2020. Short-term exposure to particulate matter (PM10 and PM2.5), nitrogen dioxide (NO2), and ozone (O3) and all-cause and cause-specific mortality: systematic review and meta-analysis. Environ. Int. 142, 105876. https://doi.org/10.1016/j.envint.2020.105876.
Pacyna, J.M., Pacyna, E.G., 2001. An assessment of global and regional emissions of trace metals to the atmosphere from anthropogenic sources worldwide. Environ. Rev. 9, 269–298. https://doi.org/10.1139/a01-012.
Panagos, P., Van Liedekerke, M., Yigini, Y., Montanarella, L., 2013. Contaminated sites in Europe: review of the current situation based on data collected through a European network. J. Environ. Public Health 2013, 1–11. https://doi.org/10.1155/2013/158764.
Paoli, L., Fačkovcová, Z., Guttová, A., 2025. Reconstructing air pollution trends in remote forests of central Europe using lichen herbarium specimens. Arch. Environ. Contam. Toxicol. 89, 34–45. https://doi.org/10.1007/s00244-025-01134-9.
Park, M., Joo, H.S., Lee, K., Jang, M., Kim, S.D., Kim, I., Borlaza, L.J.S., Lim, H., Shin, H., Chung, K.H., Choi, Y.-H., Park, S.G., Bae, M.-S., Lee, J., Song, H., Park, K., 2018. Differential toxicities of fine particulate matters from various sources. Sci. Rep. 8, 17007. https://doi.org/10.1038/s41598-018-35398-0.
Pathak, P., Srivastava, R.R., Keceli, G., Mishra, S., 2020. Assessment of the alkaline earth metals (Ca, Sr, Ba) and their associated health impacts. In: Pathak, P., Gupta, D.K. (Eds.), Strontium Contamination in the Environment, the Handbook of Environmental Chemistry. Springer International Publishing, Cham, pp. 227–243. https://doi.org/10.1007/978-3-030-15314-4_12.
Pawlik-Skowrońska, B., Di Toppi, L.S., Favali, M.A., Fossati, F., Pirszel, J., Skowroński, T., 2002. Lichens respond to heavy metals by phytochelatin synthesis. New Phytol. 156, 95–102. https://doi.org/10.1046/j.1469-8137.2002.00498.x.
Pesaresi, M., Schiavina, M., Politis, P., Freire, S., Krasnodębska, K., Uhl, J.H., Carioli, A., Corbane, C., Dijkstra, L., Florio, P., Friedrich, H.K., Gao, J., Leyk, S., Lu, L., Maffenini, L., Mari-Rivero, I., Melchiorri, M., Syrris, V., Van Den Hoek, J., Kemper, T., 2024. Advances on the global human settlement layer by joint assessment of Earth observation and population survey data. Int. J. Digit. Earth 17, 2390454. https://doi.org/10.1080/17538947.2024.2390454.
Petit, D., Véron, A., Flament, P., Deboudt, K., Poirier, A., 2015. Review of pollutant lead decline in urban air and human blood: a case study from northwestern Europe. C. R. Geosci. 347, 247–256. https://doi.org/10.1016/j.crte.2015.02.004.
Pokorná, P., Hovorka, J., Hopke, P.K., 2016. Elemental composition and source identification of very fine aerosol particles in a European air pollution hot-spot. Atmos. Pollut. Res. 7, 671–679. https://doi.org/10.1016/j.apr.2016.03.001.
Pollard, A.S., Williamson, B.J., Taylor, M., Purvis, W.O., Goossens, M., Reis, S., Aminov, P., Udachin, V., Osborne, N.J., 2015. Integrating dispersion modelling and lichen sampling to assess harmful heavy metal pollution around the Karabash copper smelter, Russian Federation. Atmos. Pollut. Res. 6, 939–945. https://doi.org/10.1016/j.apr.2015.04.003.
Probeck, M., Ruiz, I., Ramminger, G., Fourie, C., Maier, P., Ickerott, M., Storch, C., Homolka, A., Muller, S.J., Tiwari, H., Stumpf, A., Chun, S., Mattos, C., Lindmayer, A., Jahangir, F., Endara, P., Berndt, F., Dohr, M., Kapferer, W., Schleicher, C., Ralser, S., Innerbichler, F., Riffler, M., Siklar, M., Aifantopoulou, D., Paralykidis, S., Pinet, C., Jaffrain, G., di Federico, A., Corsi, M., Langanke, T., Dufourmont, H., 2021. CLC+ backbone: set the scene in copernicus for the coming decade. In: 2021 IEEE International Geoscience and Remote Sensing Symposium IGARSS. Presented at the IGARSS 2021 - 2021 IEEE International Geoscience and Remote Sensing Symposium. IEEE, Brussels, Belgium, pp. 2076–2079. https://doi.org/10.1109/IGARSS47720.2021.9553252.
Purvis, O.W., Chimonides, P.D.J., Jeffries, T.E., Jones, G.C., Rusu, A.-M., Read, H., 2007. Multi-element composition of historical lichen collections and bark samples, indicators of changing atmospheric conditions. Atmos. Environ. 41, 72–80. https://doi.org/10.1016/j.atmosenv.2006.08.040.
Purvis, O.W., Chimonides, P.J., Jeffries, T.E., Jones, G.C., Read, H., Spiro, B., 2005. Investigating biogeochemical signatures in the lichen Parmelia sulcata at Burnham

Beeches, Buckinghamshire, England. Lichenologist 37, 329–344. https://doi.org/10.1017/S0024282905015288.
R Core Team, 2024. R: a Language and Environment for Statistical Computing.
Rauch, J.N., Pacyna, J.M., 2009. Earth's global Ag, Al, Cr, Cu, Fe, Ni, Pb, and Zn cycles. Glob. Biogeochem. Cycles 23, 3376. https://doi.org/10.1029/2008GB003376.
Reid, A., Musyck, B., 2000. Industrial policy in Wallonia: a rupture with the past? Eur. Plan. Stud. 8, 183–200. https://doi.org/10.1080/096543100110820.
Rienda, I.C., Alves, C.A., 2021. Road dust resuspension: a review. Atmos. Res. 261, 105740. https://doi.org/10.1016/j.atmosres.2021.105740.
Schröder, W., Nickel, S., 2019. Spatial structures of heavy metals and nitrogen accumulation in moss specimens sampled between 1990 and 2015 throughout Germany. Environ. Sci. Eur. 31, 33. https://doi.org/10.1186/s12302-019-0216-y.
Sen, I.S., Peucker-Ehrenbrink, B., 2012. Anthropogenic disturbance of element cycles at the Earth's surface. Environ. Sci. Technol. 46, 8601–8609. https://doi.org/10.1021/es301261x.
Sloof, J.E., Wolterbeek, H.Th, 1991. National trace-element air pollution monitoring survey using epiphytic lichens. Lichenologist 23, 139–165. https://doi.org/10.1017/S0024282991000300.
Snyder, E.G., Watkins, T.H., Solomon, P.A., Thoma, E.D., Williams, R.W., Hagler, G.S.W., Shelow, D., Hindin, D.A., Kilaru, V.J., Preuss, P.W., 2013. The changing paradigm of air pollution monitoring. Environ. Sci. Technol. 47, 11369–11377. https://doi.org/10.1021/es4022602.
Sérusiaux, E., Diederich, P., Lambinon, J., 2004. Les Macrolichens De Belgique, Du Luxembourg Et Du Nord De La France. Musée d'histoire naturelle Luxembourg.
Taylor, S.R., McLennan, S.M., 1985. The Continental Crust: Its Composition and Evolution. Blackwell Scientific Publications, Oxford, UK.
Tshibangu, J.-P., Deloge, K.P.-A., Deschamps, B., Coudyzer, C., 2004. Assessment of rock slope stability in limestone quarries in the Tournai's region (Belgium) using structural data. In: Hack, R., Azzam, R., Charlier, R. (Eds.), Engineering Geology for Infrastructure Planning in Europe, Lecture Notes in Earth Sciences. Springer, Berlin Heidelberg, Berlin, Heidelberg, pp. 604–613. https://doi.org/10.1007/978-3-540-39918-6_67.
U.S. Environmental Protection Agency, 2014. Positive Matrix Factorization (PMF) 5.0 Fundamentals and User Guide (No. EPA/600/R-14/108). U.S. Environmental Protection Agency, Office of Research and DevelopmentInstitution, Washington, DC.
Vandeuren, A., Pereira, B., Kaba, A.J., Titeux, H., Delmelle, P., 2023. Environmental bioavailability of arsenic, nickel and chromium in soils impacted by high geogenic and anthropogenic background contents. Sci. Total Environ. 902, 166073. https://doi.org/10.1016/j.scitotenv.2023.166073.
Vern, M.L., 2022. Effects of soil surface degradation and vehicle momentum on dust emissions and visibility reduction from unpaved roads. Transp. Geotechn. 37, 12.
von Storch, H., Costa-Cabral, M., Hagner, C., Feser, F., Pacyna, J., Pacyna, E., Kolb, S., 2003. Four decades of gasoline lead emissions and control policies in Europe: a retrospective assessment. Sci. Total Environ. 311, 151–176. https://doi.org/10.1016/S0048-9697(03)00051-2.
Véron, A., Flament, P., Bertho, M.L., Alleman, L., Flegal, R., Hamelin, B., 1999. Isotopic evidence of pollutant lead sources in Northwestern France. Atmos. Environ. 33, 3377–3388. https://doi.org/10.1016/S1352-2310(98)00376-8.
Wang, G., Zeng, C., Zhang, F., Zhang, Y., Scott, C.A., Yan, X., 2017. Traffic-related trace elements in soils along six highway segments on the Tibetan Plateau: influence factors and spatial variation. Sci. Total Environ. 581–582, 811–821. https://doi.org/10.1016/j.scitotenv.2017.01.018.
Wolterbeek, B., 2002. Biomonitoring of trace element air pollution: principles, possibilities and perspectives. Environ. Pollut. 120, 11–21. https://doi.org/10.1016/S0269-7491(02)00124-0.
World Health Organization, 2021. WHO global air quality guidelines: particulate matter. PM2.5 and PM10), Ozone, Nitrogen Dioxide, Sulfur Dioxide and Carbon Monoxide. World Health Organization, Geneva.
Wu, L., Isley, C.F., Handley, H.K., Taylor, M.P., 2021. Atmospheric sources of anthropogenic and geogenic trace metals in Australian lichen and fungi. Anthropocene 33, 100279. https://doi.org/10.1016/j.ancene.2021.100279.
Zanobetti, A., Schwartz, J., 2009. The effect of fine and coarse particulate air pollution on mortality: a national analysis. Environ. Health Perspect. 117, 898–903. https://doi.org/10.1289/ehp.0800108.
Zevenhoven, R., Mukherjee, A., Bhattacharya, P., 2007. Arsenic flows in the environment of the European Union: a synoptic review. In: Trace Metals in the Environment. Elsevier, pp. 527–547. https://doi.org/10.1016/S0927-5215(06)09020-5.
Zhang, H., Wang, F., Zhou, S., Zhang, T., Qi, M., Song, H., 2025. Contribution of dust emissions from farmland to particulate matter concentrations in North China Plain: integration of WRF-Chem and WEPS model. Environ. Int. 195, 109191. https://doi.org/10.1016/j.envint.2024.109191.
Zhao, Lili, Zhang, C., Jia, S., Liu, Q., Chen, Q., Li, X., Liu, X., Wu, Q., Zhao, Liangcheng, Liu, H., 2019. Element bioaccumulation in lichens transplanted along two roads: the source and integration time of elements. Ecol. Indic. 99, 101–107. https://doi.org/10.1016/j.ecolind.2018.12.020.